Time-resolved fluorescence studies of tomaymycin bonding to synthetic DNAs

ARTICLE *in* BIOPHYSICAL JOURNAL · MAY 1996

Impact Factor: 3.97 · DOI: 10.1016/S0006-3495(96)79756-4 · Source: PubMed

4 AUTHORS, INCLUDING:

Mary D Barkley

Case Western Reserve University

75 PUBLICATIONS **2,928** CITATIONS

SEE PROFILE

Wanda Walczak

Corning Incorporated

8 PUBLICATIONS **60** CITATIONS

SEE PROFILE

Time-Resolved Fluorescence Studies of Tomaymycin Bonding to Synthetic DNAs

Mary D. Barkley, Qi Chen, Wanda J. Walczak, and Karol Maskos
Department of Chemistry, Louisiana State University, Baton Rouge, Louisiana 70803 USA

ABSTRACT Tomaymycin reacts covalently with guanine in the DNA minor groove, exhibiting considerable specificity for the flanking bases. The sequence dependence of tomaymycin bonding to DNA was investigated in synthetic DNA oligomers and polymers. The maximum extent of bonding to DNA is greater for homopurine and natural DNA sequences than for alternating purine-pyrimidine sequences. Saturation of DNA with tomaymycin has little effect on the melting temperature in the absence of unbound drug. Fluorescence lifetimes were measured for DNA adducts at seven of the ten unique trinucleotide bonding sites. Most of the adducts had two fluorescence lifetimes, representing two of the four possible binding modes. The lifetimes cluster around 2–3 ns and 5–7 ns; the longer lifetime is the major component for most bonding sites. The two lifetime classes were assigned to *R* and *S* diastereomeric adducts by comparison with previous NMR results for oligomer adducts. The lifetime difference between binding modes is interpreted in terms of an anomeric effect on the excited-state proton transfer reaction that quenches tomaymycin fluorescence. Bonding kinetics of polymer adducts were monitored by fluorescence lifetime measurements. Rates of adduct formation vary by two orders of magnitude with poly(dA-dG)·poly(dC-dT), reacting the fastest at 4×10^{-2} M^{-1} s^{-1}. The sequence specificity of tomaymycin is discussed in light of these findings and other reports in the literature.

INTRODUCTION

Tomaymycin is a member of the pyrrolo[1,4]benzodiazepine group of antitumor antibiotics, which includes anthramycin, sibiromycin, and the neothramycins A and B. These antibiotics react with guanine bases in the minor groove of B-form DNA (Hurley and Needham-VanDevanter, 1986). The aminal linkage between the drug C11 and guanine N2 was suggested by structure-activity relationships and model building (Petrusek et al., 1981) and confirmed by ^{1}H NMR in a bis-tomaymycin-d(CICGAATTCICG)$_2$ adduct (Boyd et al., 1990b). Formation of the DNA adduct appears to proceed by a S_N1 mechanism through the N10-C11 imine intermediate (Fig. 1). Consequently, the configuration at C11 of the carbinolamine does not influence the stereochemical outcome of the nucleophilic attack (Barkley et al., 1986). Four binding modes are possible: *R* or *S* configuration at C11 with the aromatic ring of the drug pointing toward the 3′ or 5′ end of the covalently attached DNA strand (Fig. 2). Molecular modeling shows that the minor groove can accommodate all four binding modes of tomaymycin and anthramycin with minimal distortion of the helix (Rao et al., 1986; Remers et al., 1986; Cheatham et al., 1988; Boyd et al., 1990b; Barkley et al., 1991; Remers et al., 1992).

The pyrrolo[1,4]benzodiazepines have remarkable sequence specificity for such small molecules. In addition to specific reaction with guanine, the drugs exhibit preferences for the flanking bases. Chemical footprinting with MPE-Fe(II) and 1,10-phenanthroline-copper showed protection of 3–5-base pair sequences on DNA (Hertzberg et al., 1986; Pierce et al., 1993). The sequence preference of tomaymycin and anthramycin has been determined by exonuclease III digestion, λ exonuclease digestion, and UvrABC nuclease incision assays (Hurley et al., 1988; Pierce et al., 1993). The relative reactivity of all 16 possible trinucleotide bonding sites 5′NGN was quantified by UvrABC nuclease incision analysis (Pierce et al., 1993). Although 5′AGA is the preferred bonding site for both drugs, the sequence specificities of tomaymycin and anthramycin are different. Tomaymycin clearly exhibits the highest bonding at the 5′AGA sequence, whereas anthramycin reacts almost as well at 5′AGG sites. Both drugs react strongly at 5′AGC and 5′GGA sites; tomaymycin also reacts strongly at 5′GGC and 5′TGC. However, the extent of DNA modification by tomaymycin is less than that by anthramycin at the same drug concentration in the assay. The sequence specificity of the pyrrolo[1,4]benzodiazepines has been proposed to be due to sequence-dependent variations in local DNA structure and flexibility. The x-ray structure of anthramycin bonded to d(CCAACGTTGG)$_2$, which contains two 5′TGG sites, shows a low twist angle for the T-G and G-G steps in the bonding site (Kopka et al., 1994). The low average twist of purine-purine steps in DNA would provide a good fit for the drug and explain the 5′RGR sequence preference of anthramycin. Correlation of the sequence preferences of

Received for publication 18 August 1995 and in final form 3 January 1996.

Address reprint requests to Dr. Mary D. Barkley, Department of Chemistry, Louisiana State University, Baton Rouge, LA 70808. Tel.: 504-388-2868; Fax: 504-388-3458; E-mail: barkley@chmcaf.chem.lsu.edu.

Abbreviations used: MPE, methidiumpropyl-EDTA; poly dG, poly(dG)·poly(dC); poly dAG, poly(dA-dG)·poly(dC-dT); poly dGT, poly(dG-dT)·poly(dA-dC); poly dGC, poly(dG-dC)·poly(dG-dC); poly dGm^{5}C, poly(dG-m^{5}dC)·poly(dG-m^{5}dC); R, purine nucleotide; P/D, nucleotide to drug ratio; FWHM, full-width half-maximum; POPOP, 1,4-bis(5-phenyloxazol-2-yl)benzene; BBO, 2,5-bis(4-biphenylyl)oxazole; λ_{ex}, excitation wavelength; λ_{em}, emission wavelength; T_m, melting temperature.

0006-3495/96/04/1923/10 $2.00

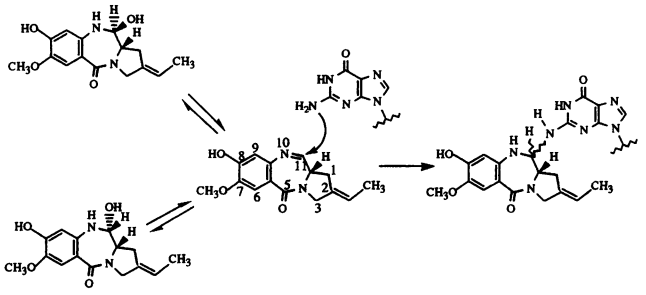

FIGURE 1 Proposed mechanism for the reaction of tomaymycin with DNA.

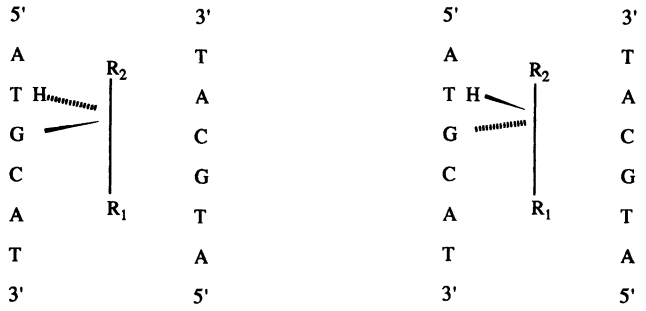

FIGURE 2 Four possible binding modes of tomaymycin.

anthramycin and tomaymycin with reaction rates and DNA bending suggests that DNA flexibility also contributes to the sequence specificity (Kizu et al., 1993).

The binding modes of tomaymycin at two sequences on duplex oligomers have been deduced from high-field NMR, molecular modeling, and fluorescence lifetime data. In the d(CICGAATTCICG)$_2$ adduct, which contains two 5′CGA sites, tomaymycin bonds with *S* configuration and 3′ orientation of the aromatic ring (Boyd et al., 1990b). However, two types of adducts are formed at the 5′TGC site in d(ATGCAT)$_2$, which were tentatively identified as the 11*S* and 11*R* diastereomers with 3′ and 5′ orientations, respectively (Cheatham et al., 1988). The relative placement of two sites has also been examined by NMR and molecular modeling as a prelude to the design of an interstrand cross-linking agent (Bose et al., 1992; Wang et al., 1992). Tomaymycin forms *S*3′ adducts at the 5′CGA and 5′AGC sites in d(CICGATCICG)$_2$ and d(CIAGCICTCG)$_2$, respectively. It appears to form at least two types of adduct in d(CITCICGACG)$_2$, presumably because of juxtaposition of the two 5′CGA sites (Wang et al., 1992). Anthramycin forms *S*3′ adducts at the 5′TGC site in d(ATGCAT)$_2$ (Boyd et al., 1990a) and the 5′TGG sites in d(CCAACGTTGG)$_2$ (Kopka et al., 1994).

Previously we showed that the 11*S* and 11*R* diastereomers of tomaymycin have different fluorescence lifetimes and slightly different absorption spectra in solution and presumably also in DNA adducts (Barkley et al., 1986). This paper presents fluorescence studies of the sequence dependence of tomaymycin bonding to DNA. The maximum extent of reaction with various synthetic DNA polymers is determined by a steady-state fluorescence assay. The fluorescence lifetimes of the polymer adducts are interpreted by comparison with results for oligomer adducts. Finally, the rates of formation for different polymer adducts are measured by time-resolved fluorescence techniques.

MATERIALS AND METHODS

Chemicals

Tomaymycin 11-methyl ether was a generous gift from Dr. M. Kohsaka (Fujisawa Pharmaceutical Co., Osaka, Japan). The buffer was 0.01 M phosphate, 0.1 M NaCl, 0.1 mM EDTA at the indicated pH. Synthetic polydeoxynucleotides (Pharmacia) were dissolved in pH 7.5 buffer. Calf thymus DNA (Sigma type I) was purified by phenol extraction and was dialyzed into pH 7.5 buffer. Nucleotide concentration was determined from the absorbance at 260 nm using the following extinction coefficients (Inman and Baldwin, 1962; Morgan and Wells, 1968; Wells et al., 1970): poly(dG)·poly(dC), 7400 M^{-1} cm^{-1}; poly(dA-dG)·poly(dC-dT), 5700 M^{-1} cm^{-1}; poly(dG-dT)·poly(dA-dC), 6500 M^{-1} cm^{-1}; poly(dG-dC)·poly(dG-dC), 8400 M^{-1} cm^{-1}; poly(dG-m^{5}dC)·poly(dG-m^{5}dC), 8400 M^{-1} cm^{-1}; calf thymus DNA, 6800 M^{-1} cm^{-1}. Oligodeoxynucleotide duplexes were provided by Dr. L. H. Hurley and were synthesized and purified as described elsewhere (Cheatham et al., 1988; Boyd et al., 1990b; Wang et al., 1992). The lyophylized samples were reconstituted with distilled water and diluted into pH 7.0 buffer or were dissolved in pH 7.0 buffer. Duplex concentration was estimated from the absorbance at 260 nm using calculated extinction coefficients as described before (Cheatham et al., 1988; Boyd et al., 1990b).

Preparation of adducts

Stock solutions of tomaymycin 11-methyl ether were prepared in methanol and were stored at −20°C. The concentration of the stock solution was determined from the absorbance at 320 nm using an extinction coefficient of 3600 M^{-1} cm^{-1} (Arima et al., 1972). An aliquot of the stock solution was placed in a vial, and the methanol was evaporated by a stream of N_2. Polynucleotide solution (1×10^{-3} M nucleotide) was added to give P/D = 100. d(AAGCTT)$_2$ and d(ATGCAT)$_2$ solutions containing 3×10^{-4} M duplex were added to give one duplex per drug. The reaction was allowed to equilibrate overnight at room temperature and then 1–2 weeks at 4°C, depending on the DNA. d(CICGATCICG)$_2$, d(CIAGCICTCG)$_2$, d(CITCICGACG)$_2$, and d(CICGAATTCICG)$_2$ adducts were provided as lyophylized samples with 0.5 duplex/drug, respectively, and were diluted to $1–3 \times 10^{-5}$ M duplex. (The concentration units of d(CICGAATTCICG)$_2$ adduct for fluorescence experiments in Boyd et al. (1990b) were nucleotides.) Solutions of DNA adducts appeared to be stable for at least 1 year when stored in the refrigerator.

Unreacted tomaymycin was removed by solvent extraction or by dialysis. Solutions of polynucleotide and calf thymus DNA adducts were extracted three or four times with an equal volume of cold, pH 7.5 buffer-saturated 2-butanol or ethyl acetate to remove free drug and two or three times with an equal volume of ether to remove 2-butanol. The ether was evaporated by bubbling N_2 through the solution. Traces of ethyl acetate were removed under vacuum. Oligonucleotide adducts were extracted similarly with pH 7.0 buffer-saturated ethyl acetate. Aliquots (1–1.5 ml) of solutions of polynucleotide and calf thymus DNA adducts were dialyzed against three 500-ml volumes of pH 7.5 buffer for 48 h at 4°C. Photobleaching under laser light was completely eliminated by scrupulous removal of O_2 as described before (Chen et al., 1994). Solutions for thermal denaturation experiments were overlaid with silicon oil. Absorbance at 260 nm was measured as a function of temperature in an Aviv 118DS spectrometer equipped with a thermoelectric cell holder.

Saturation binding was determined by a difference method, in which the amount of unbound tomaymycin was measured by fluorescence after 2-butanol extraction. Solutions of polynucleotide and calf thymus DNA adducts (2.5×10^{-4} M nucleotide, P/D = 5) in pH 7.5 buffer were equilibrated overnight at 25°C and then for 6 days at 4°C or for a second day at 25°C. A 2.1-ml volume of adduct solution and three 2.1-ml volumes of 5×10^{-5} M tomaymycin in pH 7.5 buffer were extracted three times with 5-ml volumes of pH 7.5 buffer-saturated 2-butanol at 4 or 25°C. After each extraction 4 ml of the 2-butanol phase was drawn off and the aqueous phase was extracted with ether. The fluorescence intensity of the 2-butanol phase was recorded at 337 nm excitation wavelength, 420 nm emission wavelength as described before (Barkley et al., 1991). The error in fluorescence intensity was <1.4% for the 2-butanol phases from the three tomaymycin samples in buffer. Usually >95% of the free tomaymycin was removed in the first extraction.

Fluorescence lifetime measurements

Adduct solutions were placed in 4×10 mm^2 stoppered cells. The absorbance at 330 nm with 4-mm path length was <0.15. Fluorescence lifetimes were measured at 5°C on a Photochemical Research Associates time-correlated single photon counting instrument equipped with a picosecond dye laser excitation source as described before (Chen et al., 1994). A thermoelectrically cooled Hamamatsu R2809U microchannel plate photomultiplier was used in a few experiments. Some of the lifetime measurements were made using flash lamp excitation and a T optical design. The flash lamp was filled with 1.7 atm of N_2 and operated at 20–25 kHz with 5 kV applied across a 1.5-mm electrode gap. Under these conditions the pulse width was about 1.7 ns FWHM. Excitation wavelengths were selected by interference filters (10-nm bandpass): 313 and 337 nm (micro-Coatings; Westford, MA) and 355 nm (Corion 3500 or 3600; Holliston, MA). Because the flash lamp excitation was unpolarized, a single polarizer oriented at 35°C was used on the emission side to eliminate anisotropic effects. Emission wavelengths were selected by Instruments SA H-10 monochromators (8-nm bandpass). The sample temperature was controlled by a circulating water bath.

Fluorescence decays from a sample and a reference fluorophore or lamp profile were acquired contemporaneously. Peak counts were 2.5×10^4 with laser excitation and $1–2 \times 10^4$ with the flash lamp. Counting rates were <1% of the laser excitation rate and <2% of the flash lamp excitation rate. Decay curves were stored in 512 channels of 0.06 or 0.108 ns/channel or in 1024 channels of 0.03 or 0.04 ns/channel. Solutions of POPOP (Fluka) in 75% ethanol and 0.8 M KI (containing a trace of sodium thiosulfate to retard I_3^- formation) or BBO in ethanol were used as reference fluorophore. Lifetimes of 0.21–0.32 ns for quenched POPOP and 1.28 ns for BBO were determined in separate experiments using anthracene in ethanol as the monoexponential standard. Scattering from an aqueous solution of glycogen was used for the lamp profile in experiments on poly dGC adduct with laser excitation and microchannel plate detection.

Fluorescence decay data were fitted by reference deconvolution to a sum of exponentials (Kolber and Barkley, 1986),

$$I(\lambda_{ex}, \lambda_{em}; t) = \Sigma_i\, \alpha_i(\lambda_{ex}, \lambda_{em})\exp(-t/\tau_i), \qquad (1)$$

where $\alpha_i(\lambda_{ex}, \lambda_{em})$ is the amplitude at excitation and emission wavelengths, λ_{ex} and λ_{em}, and τ_i is the fluorescence lifetime for component i. Goodness of fit was judged from the value of reduced chi-square χ_r^2 and the shape of the autocorrelation function of the weighted residuals. The reference lifetime was an adjustable parameter in analyses of the monoexponential standard. Its value was fixed in analyses of tomaymycin decays. Decay data deconvolved with a lamp profile used Eq. 1 as the fitting function. Fluorescence decay curves acquired for multiple samples at different excitation and emission wavelengths were deconvolved by single-curve analysis and by global analysis. The global analysis program assumes that the lifetimes but not the amplitudes are independent of sample treatment and wavelength (Knutson et al., 1983).

Bonding kinetics

The rate of formation of DNA adduct was monitored by fluorescence lifetime measurements using flash lamp excitation. An aliquot of tomaymycin methyl ether stock solution was placed in a cell, the methanol was evaporated, and polynucleotide solution (1×10^{-3} M nucleotide) was added to give P/D = 100. After vortexing, the cell was placed in the sample holder. Initially 30 consecutive decay curves with at least 2×10^3 peak counts were acquired at 313 nm excitation wavelength, 420 nm emission wavelength. Another 20–50 decay curves with 1×10^4 peak counts were acquired at longer times up to 1–2 weeks until there was no further change in the relative amplitude of the free drug component.

The complete set of decay curves was fitted to two or three exponentials by global analysis. Rate constants were determined from changes in relative amplitudes of the lifetime components as a function of time as described before (Chen et al., 1994). Because the reaction

$$\text{TOM} + \text{DNA} \xrightarrow{k} \text{TOM} - \text{DNA} \qquad (2)$$

was carried out with a 25- to 50-fold excess of potential DNA bonding sites, pseudo-first-order kinetics were assumed at early times. The pseudo-first-order rate constant $k' = k[\text{DNA}]_o$ was determined from the slope of the linear portion of a plot of $-\ln \alpha_f$ versus t, where α_f is the relative amplitude of the free drug decay. For a single species of DNA adduct, the rate of disappearance of free drug equals the rate of formation of drug-DNA adduct. For two species of DNA adduct formed by two concurrent reactions like Eq. 2, the rate of disappearance of free drug equals the sum of the rates of formation of the two adducts: $k' = k_1' + k_2'$. The pseudo-first-order rate constant k_i' for species i is obtained from

$$\alpha_i = k_i'/k'[1 - \exp(-k't)]. \qquad (3)$$

The rate constants k_1' and k_2' were evaluated by two methods with equivalent results: 1) k' and the amplitude ratio α_1/α_2 at equilibrium and 2) nonlinear fits of the amplitude data for the major lifetime component to Eq. 3. Nonlinear fits of the amplitude data for the minor component gave less satisfactory results.

RESULTS

Synthetic DNA adducts

The absorption and fluorescence emission spectra of tomaymycin bonded to guanine-containing synthetic DNA polymers are similar to the spectra of the calf thymus DNA adduct (Barkley et al., 1991). Table 1 lists the absorption and emission maxima of the synthetic DNA adducts.

TABLE 1 Properties of tomaymycin-polynucleotide adducts

Polynucleotide	λ_{abs}^{max} (nm)	λ_{em}^{max} (nm)	Saturation ratio* (nucleotide/drug)
Poly(dG) · poly(dC)	329	406	17.4 (25.8)
Poly(dA-dG) · poly(dC-dT)	327	410	18.4 (17.9)
Poly(dG-dT) · poly(dA-dC)	327	407	27.8 (41.0)
Poly(dG-dC) · poly(dG-dC)	329	409	28.2 (39.6)
Poly(dG-m^{5}dC) · poly(dG-m^{5}dC)‡	326	413	42.6 (120.8)
Calf thymus DNA	330	407	17.2 (18.7)

pH 7.5, 5°C, [P] = 1×10^{-3} M. Absorption and emission spectra were measured on samples with P/D = 100. Free drug was removed by extraction or dialysis.

*Amount of drug bonded at saturation was determined as described in Materials and Methods. Data for 25°C in parentheses.

‡Free drug was not removed before measuring spectra.

The maximum extent of bonding to synthetic DNA polymers was measured at 5 and 25°C by a fluorescence assay. Assuming the drug molecule covers a minimum of three base pairs and every base pair begins a potential bonding site, the DNA would saturate at three base pairs per drug or P/D = 6. The synthetic DNA polymers were reacted with excess tomaymycin at P/D = 5. Unreacted drug was removed by extraction and quantified by fluorescence. The fraction of tomaymycin bonded to DNA was determined by comparison of identical samples with and without DNA. A nucleotide-to-drug ratio of 18.7 was obtained for calf thymus DNA at pH 7.5, 25°C. This compares to a value of 18.2 determined by radiometric assay at pH 7.2, 22°C (Hurley et al., 1977). Table 1 gives the results for five synthetic DNA polymers. At 5°C the two homopurine sequences, poly dG and poly dAG, bond tomaymycin to the same extent as calf thymus DNA: 18 nucleotides per drug. The copolymer sequences poly dGC and poly dGT saturate at 28 nucleotides per drug, whereas the methylated sequence poly dGm^{5}C saturates at 42 nucleotides per drug. The saturation ratios are larger at 25°C, except in the case of poly dAG and calf thymus DNA.

The melting temperatures of synthetic DNA polymers saturated with tomaymycin were also determined. After extraction of free drug, the adduct solutions were diluted eightfold with water to give a final [Na^+] = 14.5 mM. The bound tomaymycin increased the T_m of poly dG, poly dAG, poly dGT, and calf thymus DNA by about 1°. The T_m of poly dGC and poly dGm^{5}C was >100°C with and without antibiotic. Previously, Nishioka et al. (1972) reported a 13° increase in the melting temperature of *Escherichia coli* DNA measured in the presence of a 40-fold excess of tomaymycin over the saturation ratio (P/D = 0.44). The T_m of calf thymus DNA increased by only 9° for a ninefold excess of tomaymycin over the saturation ratio (P/D = 2). Apparently the presence of unreacted antibiotic stabilizes the DNA helix against thermal denaturation.

Lifetimes of polymer adducts

Fluorescence decays of synthetic DNA adducts were acquired at various excitation and emission wavelengths. Measurements were made at 5°C on samples equilibrated at P/D = 100 before and after solvent extraction or dialysis to remove free tomaymycin. The decay curves were deconvolved in single-curve and multiple-curve analyses. Decay curves for each synthetic DNA under different experimental conditions plus a free tomaymycin decay curve were analyzed globally with the lifetimes linked. Table 2 presents the results of global analyses of one or more samples. Only relative amplitudes and lifetimes for the DNA adducts are given. At 5°C the lifetime of free tomaymycin was 1.1 ns. The amount of unreacted tomaymycin at equilibrium was estimated from the amplitude of the 1.1 ns decay. In a mixture of fluorophores the relative amplitude of component i is

$$\alpha_i(\lambda_{ex}, \lambda_{em}) = \epsilon_i(\lambda_{ex}) I_i(\lambda_{em}) k_{r,i} c_i, \quad (4)$$

where $\epsilon_i(\lambda_{ex})$ is the molar extinction coefficient, $I_i(\lambda_{em})$ is the fluorescence emission spectrum, $k_{r,i}$ is the radiative rate, and c_i is the concentration. The emission spectra and radiative rates are almost the same for free and bound tomaymycin, and their relative absorbance (free/bound) is about 1.5 at 313 nm and 0.42 at 337 nm (Barkley et al., 1991). In equilibrated samples with P/D = 100 at 5°C the fraction of free drug was roughly 20% for poly dG and poly dGm^{5}C, but only 10% for poly dAG, poly dGT, and poly dGC.

The poly dG adduct has a single fluorescence lifetime of 7.2 ns. The fluorescence decays were best fit by double exponentials in single- and multiple-curve analyses. One component had a lifetime of 1.15–1.18 ns, greater amplitude at 313 nm excitation wavelength than at 337 or 355 nm, and smaller amplitude in extracted or dialyzed samples compared to equilibrated samples. This component was assigned to free tomaymycin.

The other polynucleotide adducts have two fluorescence lifetimes: 7.2 and 4.8 ns for poly dAG, 5.3 and 3.1 ns for poly dGT, 7.5 and 4.6 ns for poly dGC, and 7.6 and 4.7 ns for poly dGm^{5}C. Although it was difficult to resolve the closely spaced biexponential decay of these DNA adducts in the presence of small amounts of free tomaymycin, there was clear evidence for two species of DNA adduct. For example, in the case of poly dGC adduct (Fig. 3), the fluorescence decays of extracted sample gave poor fits to a single exponential with χ^2_r = 29 and a lifetime of 6.6 ns. Double exponential fits of these data gave a χ^2_r value of 6.9 with lifetimes of 6.9 and 0.5 ns. It was possible to resolve a

TABLE 2 Fluorescence lifetime data for tomaymycin-polynucleotide adducts

Polynucleotide	λ_{ex} (nm)	α_1	τ_1 (ns)	τ_2 (ns)	χ^2_r
Poly(dG) · poly(dC)*		1.00	7.2		1.4
Poly(dA-dG) · poly(dC-dT)‡	333	0.63 ± 0.05	7.2	4.8	1.6
Poly(dG-dT) · poly(dA-dC)§	313	0.83 ± 0.02	5.3	3.1	1.2
	337	0.88 ± 0.02			
	355	0.93 ± 0.01			
Poly(dG-dC) · poly(dG-dC)¶	332	0.82 ± 0.01	7.5	4.6	1.8
Poly(dG-m^{5}dC) · poly(dG-m^{5}dC)‖	313	0.88 ± 0.03	7.6	4.7	1.0
	337	0.90 ± 0.01			
	355	0.94 ± 0.01			

pH 7.5, 5°C, [P] = 1 × 10^{-3} M, P/D = 100. Global analysis of data acquired at the indicated λ_{ex} and λ_{em} = 400–420 nm (5- or 10-nm intervals).

*Three samples: equilibrated, extracted, and dialyzed. Results from fit to two exponentials with free drug component subtracted.

‡Extracted sample. Results from fit to four exponentials with free drug component (1.04 ns) and stray laser light (30 ps) subtracted.

§Four samples: equilibrated for 2 and 6 weeks, extracted, and dialyzed. Results from fit to three exponentials with free drug component subtracted.

¶Extracted sample. Results from fit to four exponentials with free drug component (1.05 ns) and stray laser light (45 ps) subtracted.

‖Four equilibrated samples. Results from fit to three exponentials with free drug component subtracted.

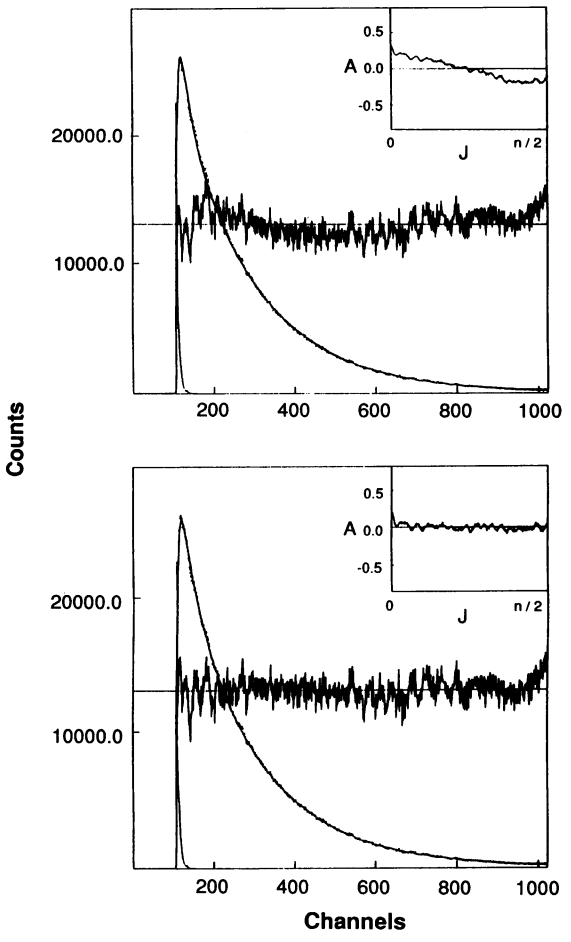

FIGURE 3 Fluorescence decay of tomaymycin-poly dGC adduct. λ_{ex} = 332 nm, λ_{em} = 400 nm, 0.040 ns/channel. pH 7.5, 5°C, [P] = 1×10^{-3} M, P/D = 100, extracted sample. Results from global analysis of data acquired at λ_{ex} = 332 nm and λ_{em} = 400–420 nm (5-nm intervals), including a decay curve for tomaymycin. Sharp spike is lamp profile. Noisy curve is sample decay; smooth curve is best fit to (*top*) three exponentials, $\alpha_1 = 0.36$, $\tau_1 = 7.04$ ns, $\alpha_2 = 0.12$, $\tau_2 = 1.05$ ns, $\alpha_3 = 0.53$, $\tau_3 = 0.035$ ns; global $\chi^2_r = 2.8$, and (*bottom*) four exponentials, $\alpha_1 = 0.28$, $\tau_1 = 7.52$ ns, $\alpha_2 = 0.11$, $\tau_2 = 4.58$ ns, $\alpha_3 = 0.08$, $\tau_3 = 1.05$ ns, $\alpha_4 = 0.52$, $\tau_4 = 0.045$ ns; global $\chi^2_r = 1.8$. Weighted percentage residuals and autocorrelation function of the residuals (*inset*) are also shown.

triple exponential with one lifetime corresponding to free drug by including a tomaymycin decay curve in the global analysis. A four exponential fit improved the χ^2_r value to 1.8 and resolved a minor species of poly dGC adduct along with a 30–50-ps component for stray laser light. The longer lifetime component constitutes the major species of these polynucleotide adducts. As seen in Table 2, the relative amplitude of the major component is independent of emission wavelength, so the emission spectra of the two species are the same. However, the amplitude of the major component increases with excitation wavelength in poly dGT and poly dGm^{5}C adducts. This shows that the absorption spectra of the two species are different, with the major component absorbing slightly to the red of the minor component.

Lifetimes of oligomer adducts

Table 3 lists the fluorescence decay parameters of six oligomer duplex adducts. In the hexamer sequences, bonding at guanine on one strand blocks the site on the other strand, so that only one drug molecule bonds per duplex. In the decamer and dodecamer sequences, the two sites are far enough apart to fit two drug molecules per duplex, one at the internal guanine on each strand. Terminal guanine is not a bonding site. The hexamers AAGCTT and ATGCAT form two species of adduct. In the AAGCTT adduct, the longer lifetime component is the major species and the absorption spectra of the two components are almost identical. However, in the ATGCAT adduct, the two lifetime components are present in roughly equal amounts and the spectrum of the 5.7-ns component is blueshifted relative to the 2.3-ns component. Two binding modes were observed by NMR for ATGCAT and assigned to *S*3′ and *R*5′ adducts, although the population of the two diastereomers was not deduced (Cheatham et al., 1988).

One decamer sequence, CICGATCICG, forms a single adduct with a 5.6-ns lifetime. NMR also showed a single

TABLE 3 Fluorescence lifetime data for tomaymycin-oligonucleotide adducts

Oligonucleotide	λ_{ex} (nm)	α_1	τ_1 (ns)	τ_2 (ns)	χ^2_r
d(AAGCTT)$_2$*	313	0.70 ± 0.01	5.1	2.9	1.2
	337	0.70 ± 0.03			
	355	0.64 ± 0.01			
d(ATGCAT)$_2$‡	313	0.60 ± 0.02	5.7	2.3	1.1
	337	0.51 ± 0.02			
	355	0.36 ± 0.01			
d(CICGATCICG)$_2$§		1.00	5.6		1.3
d(CIAGCICTCG)$_2$¶	318	0.89 ± 0.01	5.4	2.6	1.35
	323	0.95 ± 0.01			
	328	0.96 ± 0.01			
	333	0.99 ± 0.01			
d(CITCICGACG)$_2$¶	318	0.640 ± 0.003	5.6	1.4	1.3
	323	0.726 ± 0.002			
	328	0.796 ± 0.003			
	333	0.825 ± 0.005			
d(CICGAATTCICG)$_2$‖		1.0	6.4		1.09
	313	0.917 ± 0.002	6.5	2.9	1.05
	337	0.94 ± 0.01			
	355	0.964 ± 0.006			

pH 7.0, 5°C. Global analysis of data acquired at indicated λ_{ex} and λ_{em}.
*λ_{em} = 410, 420, and 430 nm. Two samples: extracted and 10-fold dilution of extracted sample equilibrated for 24 h. Results from fit to three exponentials with free drug component subtracted. Amplitudes are mean values from extracted sample.
‡λ_{em} = 410 and 420 nm. Extracted sample. Results from fit to three exponentials with free drug component subtracted.
§λ_{ex} = 313, 323, 328, and 333 nm; λ_{em} = 395–415 nm (5-nm intervals). Extracted sample.
¶λ_{em} = 395–415 nm (5-nm intervals). Extracted sample.
‖λ_{em} = 400–440 nm (10-nm intervals). Seven samples: equilibrated for 4 weeks, threefold dilution before and after extraction, and 6-, 12-, 24-, and 48-fold serial dilutions of extracted sample equilibrated for 24 h after each dilution. Results from fits to two and three exponentials with free drug component subtracted. Amplitudes are mean values from threefold diluted sample before and after extraction.

species of adduct with *S3′* binding mode (Wang et al., 1992). The other decamers, CIAGCICTCG and CITCICGACG, form two species of adduct. The major component has a lifetime of 5.4–5.6 ns and a redshifted absorption spectrum. For the CIAGCICTCG adduct, NMR showed a single *S3′* binding mode (Wang et al., 1992). Presumably, the amount of minor lifetime component present is too low (<10%) to detect by NMR. However, for the CITCICGACG adduct, NMR indicated more than one binding mode, at least one of which has *S* configuration (Wang et al., 1992). The observation of multiple binding modes in the CITCICGACG sequence was attributed to the proximity of the two 5′CGA bonding sites. The dodecamer sequence CICGAATTCICG appears to form a single species of adduct with a 6.4-ns lifetime. Global analysis of data for equilibrated, extracted, and diluted samples plus free tomaymycin gave an excellent fit to a double exponential with a free drug lifetime of 1.18 ns. Although it was possible to resolve a triple exponential with a 1.18-ns lifetime for the free drug, the evidence for a minor 2.9-ns component is weak. There is no improvement in the global χ^2_r, or autocorrelation function between the double and triple exponential fits. Moreover, the amplitude of the 1.18-ns decay in the triple exponential fit does not show the excitation wavelength dependence characteristic of free tomaymycin. A single *S3′* binding mode for CICGAATTCICG adduct was observed by NMR (Boyd et al., 1990b).

Table 4 summarizes the lifetime data for the synthetic polymer and oligomer adducts. The bonding sequences include seven of the ten unique of 16 possible trinucleotide sites on natural DNA. The lifetimes span a 6-ns range from 1.4 to 7.6 ns, with clusters around 2–3 ns and 5–7 ns. NMR identifies the 5.6- and 6.4-ns lifetimes of the 5′CGA bonding sites as the *S3′* binding mode. This suggests that the 5–7-ns lifetime group represents *S3′* adduct and assigns the 5.7-ns lifetime of the 5′TGC site to the *S3′* binding mode and the 2.3-ns lifetime to the *R5′* binding mode. We argue that the 2–3-ns lifetime group represents *R5′* adduct.

Bonding kinetics

Fluorescence lifetime data were acquired at 313 nm excitation wavelength and 420 nm emission wavelength as a function of time after mixing tomaymycin and synthetic DNA polymer. The decay curves from the kinetics experiment were deconvolved simultaneously with a free tomaymycin decay curve. Fig. 4 depicts the time course of the relative amplitudes of the free drug decay and the two lifetime components of the poly dGC adduct. The amplitude of each species is proportional to its concentration. The rate constants for formation of DNA adducts were calculated assuming pseudo-first-order kinetics. Table 5 gives the pseudo-first-order rate constants measured at 1×10^{-3} M nucleotide as well as bimolecular rate constants estimated using the guanine nucleotide concentration. The rates of adduct formation are slow and vary by two orders of magnitude among adducts. Poly dAG reacts the fastest, with an overall bimolecular rate constant of $4 \times 10^{-2}\ M^{-1}\ s^{-1}$. The minor species of the poly dGC and poly dGm^{5}C adducts are the slowest to form, with rate constants of $2–4 \times 10^{-4}\ M^{-1}\ s^{-1}$. The reaction of pyrrolo[1,4]benzodiazepines with DNA is acid catalyzed, and the rate is proportional to hydrogen ion concentration (Kohn et al., 1970, 1974). Decreasing the pH from 7.5 to 5.5 increases the rate about 100-fold. According to the proposed mechanism (Fig. 1), the acid-catalyzed step is formation of the imine intermediate. The imine is nonfluorescent. Presumably, the overall reaction involves association of the imine with DNA followed by covalent reaction. However, noncovalent bonding of the drug to DNA would not be detected by fluorescence. For example, the fluorescence lifetime of tomaymycin does not change in the presence of poly(dI-dC), which lacks the amino group at the 2 position of the purine ring.

TABLE 4 Tomaymycin lifetimes at 5′NGN bonding sites

Bonding sequence	τ_1 (ns)	τ_2 (ns)	Context
GGG	7.2		Polymer
AGA	7.2	4.8	Polymer
AGC	5.1	2.9	Hexamer
	5.4	2.6	Decamer
CGA	5.6		Decamer
	5.6	1.4	Decamer
	6.4		Dodecamer
TGC	5.7	2.3	Hexamer
TGT	5.3	3.1	Polymer
CGC	7.5	4.6	Polymer
m^{5}CGm^{5}C	7.6	4.7	Polymer

Data from Tables 2 and 3.

DISCUSSION

The fluorescence lifetime is governed by the radiative k_r and nonradiative k_{nr} rates:

$$\tau^{-1} = k_r + k_{nr}. \quad (5)$$

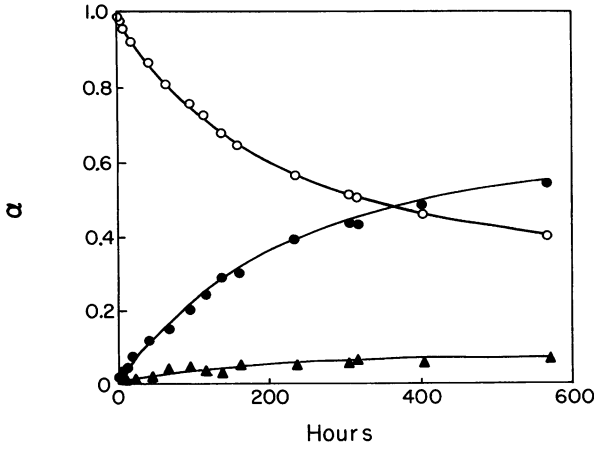

FIGURE 4 Kinetics of formation of tomaymycin-poly dGC adduct. λ_{ex} = 313 nm, λ_{em} = 420 nm, pH 7.5, 5°C, [P] = 1×10^{-3} M, P/D = 100. Results from global fit to three exponentials, χ^2_r = 1.11. ○, free tomaymycin; ●, major component; ▲, minor component.

TABLE 5 Kinetics of formation of tomaymycin-polynucleotide adducts

Polynucleotide	$k' \times 10^6$ (s^{-1})	$k'_1 \times 10^6$ (s^{-1})	$k_1 \times 10^3$ ($M^{-1}s^{-1}$)	$k'_2 \times 10^6$ (s^{-1})	$k_2 \times 10^3$ ($M^{-1}s^{-1}$)
Poly(dG) · poly(dC)	0.5	0.5	1.0		
Poly(dA-dG) · poly(dC-dT)*	11	11	44.0		
Poly(dG-dT) · poly(dA-dC)	1.1	0.8	3.2	0.3	1.2
Poly(dG-dC) · poly(dG-dC)	1.0	0.9	1.8	0.1	0.2
Poly(dG-dm^5C) · poly(dG-dm^5C)	2.3	2.1	4.2	0.2	0.4

pH 7.5, 5°C, [P] = 1×10^{-3} M, P/D = 100. Pseudo-first-order rate constant k'_i and bimolecular rate constant k_i of lifetime component i; major component $i = 1$, minor component $i = 2$. $k'_i = k_i$[site], where each G is considered a potential bonding site.
*Results from fit to two exponentials assuming a single species of adduct.

The radiative rate of tomaymycin is not very sensitive to environment (Barkley et al., 1986, 1991). The lifetime differences among binding modes and bonding sites are due largely to the nonradiative rate. Two nonradiative processes have been shown to occur in tomaymycin: intersystem crossing and excited-state proton transfer. The low-temperature luminescence spectrum of tomaymycin ethyl ether in an ethanol glass has two peaks (data not shown). The total luminescence yield is 0.99 ± 0.01, and the ratio of phosphorescence to fluorescence quantum yields is 1.2 ± 0.2. The radiative rate calculated from the fluorescence quantum yield and average lifetime for calf thymus DNA adduct is about 7×10^7 s^{-1} (Barkley et al., 1986). We estimate an intersystem crossing rate for DNA adduct of about 8×10^7 s^{-1} by assuming a ratio of 1.2 for the intersystem crossing and radiative rates. Excited-state proton exchange occurs at C6 and C9 of the free drug in protic solvents (Chen et al., 1995). In the DNA adduct, the aromatic ring of tomaymycin is buried in the minor groove with C9 facing the floor of the groove and C6 exposed to solvent; proton transfer from solvent is only expected to occur at C6. Assuming that intersystem crossing is not environmentally sensitive, the proton transfer rate would determine the lifetime differences in various species of DNA adduct.

The proton transfer rate depends on the proximity of proton donors to tomaymycin in the DNA adduct. Dynamical fluctuations that change the distance between tomaymycin and putative proton donors should result in a distribution of fluorescence lifetimes. Fluorescence decay data for calf thymus DNA adduct have been analyzed for lifetime distributions (Chen et al., 1994). At low bonding density, the preferred lifetime model is a discrete double exponential, arguing against fluctuational motions at the DNA binding site. However, initial anisotropies from time-resolved experiments of tomaymycin-DNA adducts differ from the steady-state anisotropy of tomaymycin in ethanol glass, suggesting that the drug may wobble with respect to DNA.

The lifetime difference between the 11*R* and 11*S* diastereomers of tomaymycin methyl ether has been attributed to an anomeric effect on the excited-state proton transfer rate (Chen et al., 1995). The anomeric effect may be defined as the sensitivity of conformation and/or reactivity to the stereoelectronics of substituents (Carey and Sundberg, 1990). In tomaymycin methyl ether, for example, the antiperiplanar overlap between the N10-C11 bond and the adjacent oxygen lone pair in the most populated conformer of the *S* diastereomer lengthens the N10-C11 bond and allows resonance structures that enhance proton transfer at aromatic carbons, thereby decreasing the fluorescence lifetime. The analogous anomeric effect in DNA adduct would occur when the lone pair on guanine N2 is antiperiplanar with the tomaymycin N10-C11 bond (Fig. 5). This torsion is prescribed by the tomaymycin N10-C11 guanine N2-C2 and tomaymycin N10-C11 guanine N2-H torsions. Analysis of energy minimized structures of the four different binding modes in ATGCAT adducts (Barkley et al., 1991) shows that the anomeric effect decreases in the order *R*3′ > *R*5′ > *S*5′ > *S*3′. A larger anomeric effect in the *R* diastereomeric adducts is opposite that of the free drug and suggests that *S* diastereomeric adducts have a longer lifetime than *R* diastereomeric adducts. This is consistent with assignment of the 5.7-ns lifetime to the *S*3′ adduct and the 2.3-ns lifetime to the *R*5′ adduct of ATGCAT (Cheatham et al., 1988). The minimized structure of the *S*5′ adduct of $(Gm^5C)_{10}$ gives a smaller anomeric effect than the *S*3′ ATGCAT adduct. If the 7.6-ns lifetime of the Gm^5C polymer adduct were assigned to the *S*5′ binding mode, then the anomeric effect could rationalize a longer lifetime in comparison to the *S*3′ ATGCAT adduct. The excess of protons in the minor groove (Lamm and Pack, 1990; Hanlon and Pack, 1994)

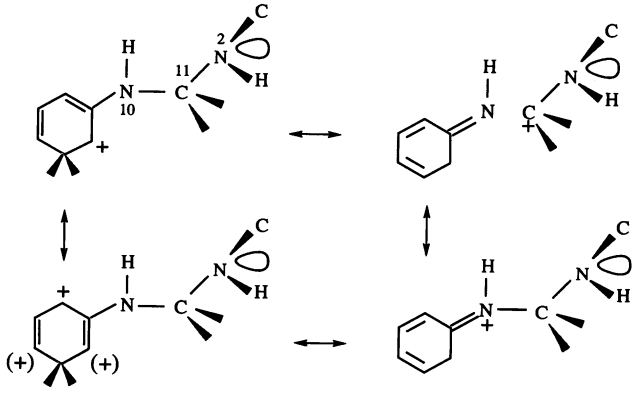

FIGURE 5 Illustration of the anomeric effect for the tomaymycin-DNA adduct, showing the tomaymycin N10-C11 guanine N2-C torsion.

may be involved in proton transfer to the aromatic ring of tomaymycin in DNA adducts.

The magnitude of the anomeric effect decreases with increasing dielectric constant of the medium (Carey and Sundberg, 1990). The dielectric constant of about 20 in the DNA minor groove (Jin and Breslauer, 1988) is modulated by the dipole moments of bases adjacent to the bonding site. The dipole moments of guanine and cytosine are about 2–3 times larger than the dipole moments of adenine and thymine (DeVoe and Tinoco, 1962), causing the dielectric constant to be locally higher in the proximity of G or C bases compared to A or T bases. Because the anomeric effect decreases the fluorescence lifetime by increasing the proton transfer rate, the lifetimes of adducts with G or C adjacent to the modified guanine are expected to be longer. Bonding sequences such as GGG, CGC, and m^5CGm^5C have the longest lifetimes (Table 4), supporting this line of reasoning.

The pyrrolo[1,4]benzodiazepines bond to B-DNA with relatively minor distortion of the helix. Tomaymycin appears to perturb DNA structure more than does anthramycin. The x-ray structure of anthramycin-d(CCAACGTTGG)$_2$ adduct has normal minor groove width and propeller twist, but ±10° helical twist changes compared to uncomplexed decamer structures (Kopka et al., 1994). ^1H and ^{31}P NMR studies of anthramycin-d(ATGCAT)$_2$ adduct show B-type sugar conformation and backbone perturbations at the two phosphates on the 5′ side of the covalently modified guanine and the cytosine of the unmodified strand. Tomaymycin-d(CICGAATTCICG)$_2$ adduct has modest perturbations in sugar conformation, the most substantial of which occurs at the covalent attachment site and its 5′ nucleoside, and in one phosphate on the 5′ side of the modified guanine. Chemical and enzymatic probes also provide evidence for drug-induced changes in DNA conformation (Hertzberg et al., 1986; Kizu et al., 1993). MPE·Fe(II) cleavage is enhanced in AT-rich regions near drug-bonding sites. Tomaymycin but not anthramycin alters the specificity of the methylene blue cleavage reaction and causes additional strand breakages three bases away from the covalently modified guanine. Both drugs inhibit hydroxyl radical cleavage and make a DNase I footprint, with tomaymycin having the larger effect. Finally, both drugs induce bending of DNA as determined by electrophoretic analysis of ligated oligomers containing unique drug-bonding sites (Kizu et al., 1993). Tomaymycin bends the DNA about 11° at all five sites tested, whereas anthramycin causes about 7° bending at two sites and no bending at the other three sites.

These subtle DNA conformation changes are probably responsible for the variations in saturation level with pyrrolo[1,4]benzodiazepine and DNA sequence. Neither anthramycin nor tomaymycin fills all possible bonding sites on natural or synthetic DNAs. Presumably, bonding of drug is limited by the energetic cost of deforming the DNA. Depending on the size taken for the bonding site, the maximum coverage would be one drug per 3 to 5 base pairs or P/D = 6 to 10. Anthramycin induces less distortion and saturates calf thymus DNA at higher binding density (P/D = 13) than does tomaymycin (P/D = 18). Tomaymycin saturates calf thymus DNA and homopurine sequences at higher binding density (P/D = 18) than alternating copolymer sequences (P/D = 28). This suggests that the conformational changes are greater in the alternating copolymers than in natural DNA and homopurine sequences. DNA bending measurements, on the other hand, indicate about the same amount of tomaymycin-induced bending at 5′AGA and 5′CGC sites (Kizu et al., 1993).

The origin of the sequence specificity of tomaymycin remains elusive. Kizu et al. (1993) found that sequence specificity correlated with greater DNA bending and faster bonding kinetics for anthramycin. Table 6 summarizes the trinucleotide sequence specificity of tomaymycin based on UvrABC nuclease incision analysis (Pierce et al., 1993). For tomaymycin, sequence specificity correlates with bonding kinetics, but not with DNA bending. 5′AGA is preferred over all possible sites by at least twofold. 5′TGT is 10-fold less reactive, whereas 5′CGC and 5′GGG are about 20-fold less reactive. The order of bonding kinetics for these sites on synthetic polynucleotides is polydAG ≫ polydGT > polydGC > polydG. Tomaymycin bonds 10-fold more slowly to polydGT, 22-fold more slowly to polydGC, and 44-fold more slowly to polydG compared to polydAG. The correlation between sequence specificity and reaction rate is hardly surprising. The UvrABC nuclease incision analysis was performed on DNA samples after reacting with tomaymycin for 3 h at 25°C, not enough time for equilibration. Therefore, the sequence specificity determined in the nuclease incision assay is essentially a single time-point measurement of the relative reaction kinetics. In the case of tomaymycin, there appears to be little if any correlation between reactivity and deformability of bonding sites. The bending

TABLE 6 Relative preferences of tomaymycin for 5′NGN bonding sites

	Observed			
	Third base			
First base	A	G	T	C
A	111 ± 54 (5)	24 ± 17 (6)	26 ± 19 (5)	47 ± 18 (8)
G	31 ± 29 (5)	4 ± 4 (4)	6 ± 6 (4)	45 ± 23 (12)
T	24 ± 21 (6)	12 ± 6 (3)	10 ± 5 (3)	44 ± 9 (8)
C	5 ± 3 (8)	13 ± 10 (10)	6 ± 2 (4)	6 ± 2 (11)

Calculated: $a = 4.2$, $b = 2.6$, $y = 3.8$, $z = 2.6$

	Third Base			
First base	A	G	T	C
A	105 (*abyz*)	40 (*aby*)	41 (*ayz*)	16 (*ay*)
G	28 (*abz*)	11 (*ab*)	11 (*az*)	4 (*a*)
T	25 (*byz*)	10 (*by*)	10 (*yz*)	4 (*y*)
C	7 (*bz*)	3 (*b*)	3 (*z*)	1 (1)

Observed data from Pierce et al. (1993). Relative intensities of UvrABC excision bands from three DNA fragments with a total of 614 base pairs. Numbers in parentheses are number of occurences of each bonding site. Calculated values for model proposed in Kopka et al. (1994). Letters in parentheses are parameters of the model as described in the text.

angle induced by tomaymycin at 5′AGA and 5′CGC sites is the same (Kizu et al., 1993), despite a 20-fold difference in reactivity. Saturation level is another measure of DNA deformation. The saturation levels of the homopurine sequences polydG and polydAG are the same, but the reactivity differs over 40-fold.

Kopka et al. (1994) proposed a model for the sequence specificity of anthramycin based on the x-ray structure of anthramycin-d(CCAACGTTGG)$_2$ adduct. This model tests the importance of purine-purine steps and A·T base pairs in specificity. For each 5′NGN trinucleotide, a four-factor product is constructed. Factors a and b weight the importance of 5′NG or GN3′ being a purine-purine step, and factors y and z weight the importance of 5′N or N3′ being A·T base pairs. The importance of each parameter is gauged by how much greater it is than 1. The four parameters were fitted to the sequence specificity data of Pierce et al. (1993) by minimizing the sum of squares of residuals over all 16 entries. The error sum has a global minimum at $a = 4.2$, $b = 2.6$, $y = 3.8$, and $z = 2.6$, yielding the calculated sequence preferences given in Table 6. This analysis suggests that tomaymycin favors purine steps and A·T base pairs on the 5′ side of the guanine bonding site relative to the 3′ side. Futhermore, purine steps are slightly more favored than A·T base pairs on the 5′ side but equally favored on the 3′ side. However, this model misses the strong preference for C on the 3′ side.

The preference of tomaymycin for purine-purine steps or A·T base pairs may be explained as follows. The absence of a 2-NH_2 group on adenine makes the minor groove significantly deeper and better able to accommodate the drug molecule, whereas guanine 2-NH_2 groups push the drug away from the floor of the groove. For guanine-binding drugs such as the pyrrolo[1,4]benzodiazepines, A·T base pairs adjacent to the bonding site allow more room for the head or tail of the drug and may account for the preference for an AGA bonding site. Purine-purine steps exhibit low helical twist angles (Yanagi et al., 1991). The normals between the five- and six-membered rings of tomaymycin make a 9° angle (Arora, 1981) in comparison to a 35.4° angle between normals in anthramycin (Mostad et al., 1978; Arora, 1979). For anthramycin, the small helical twist provided by purine-purine steps is always more important than the room provided by A·T base pairs adjacent to the binding site, even though the acrylamide tail in anthramycin is longer than the ethylidene tail in tomaymycin. In the minor groove, the position and type of hydrogen bonds do not change if base pairs are flipped, as in T·A and A·T. Thus if hydrogen bonding patterns were important in drug specificity, then TGT and AGA sites would be equally preferred. This is clearly not the case, as AGA sites are 10-fold more reactive than TGT sites. Nevertheless, as suggested by molecular modeling studies of tomaymycin-d(ATGCAT)$_2$ adducts, different binding modes may have different hydrogen bonding patterns between tomaymycin and DNA bases or water molecules in the minor groove, which may promote or deter the formation of certain adducts (Cheatham et al., 1988; Barkley et al., 1991).

We thank Dr. W. A. Remers for the coordinates of energy minimized structures of tomaymycin-DNA adducts.

This work was supported by NIH grant GM35009.

REFERENCES

Arima, K., M. Kohsaka, G. Tamura, H. Imanaka, and H. Sakai. 1972. Studies on tomaymycin, a new antibiotic. I. Isolation and properties of tomaymycin. *J. Antibiot.* 25:437–444.

Arora, S. K. 1979. Structural investigations of mode of action of drugs. II. Molecular structure of anthramycin, tomaymycin, and sibiromycin. *Acta Crystallogr.* B35:2945–2948.

Arora, S. K. 1981. Structure of tomaymycin, a DNA binding antitumor antibiotic. *J. Antibiot.* 34:462–464.

Barkley, M. D., S. Cheatham, D. E. Thurston, and L. H. Hurley. 1986. Pyrrolo[1,4]benzodiazepine antitumor antibiotics: evidence for two forms of tomaymycin bound to DNA. *Biochemistry.* 25:3021–3031.

Barkley, M. D., T. J. Thomas, K. Maskos, and W. A. Remers. 1991. Steady-state fluorescence and molecular-modeling studies of tomaymycin-DNA adducts. *Biochemistry.* 30:4421–4431.

Bose, D. S., A. S. Thompson, J. Ching, J. A. Hartley, M. D. Berardini, T. C. Jenkins, S. Neidle, L. H. Hurley, and D. E. Thurston. 1992. Rational design of a highly efficient irreversible DNA interstrand cross-linking agent based on the pyrrolobenzodiazepine ring system. *J. Am. Chem. Soc.* 114:4939–4941.

Boyd, F. L., S. F. Cheatham, W. Remers, G. C. Hill, and L. H. Hurley. 1990a. Characterization of the structure of the anthramycin-d(ATGCAT)$_2$ adduct by NMR and molecular modeling studies. Determination of the stereochemistry of the covalent linkage site, orientation in the minor groove of DNA, and effect on local DNA structure. *J. Am. Chem. Soc.* 112:3280–3289.

Boyd, F. L., D. Stewart, W. A. Remers, M. D. Barkley, and L. H. Hurley. 1990b. Characterization of a unique tomaymycin-d(CICGAATTCICG)$_2$ adduct containing two drug molecules per duplex by NMR, fluorescence, and molecular modeling studies. *Biochemistry.* 29:2387–2403.

Carey, F. A., and R. I. Sundberg. 1990. Advanced Organic Chemistry, Part A, Structure and Mechanisms, 3rd ed. Plenum Press, New York.

Cheatham, S., A. Kook, L. H. Hurley, M. D. Barkley, and W. Remers. 1988. One- and two-dimensional NMR, fluorescence, and molecular modeling studies on the tomaymycin-d(ATGCAT)$_2$ adduct. Evidence for two covalent adducts with opposite orientations and stereochemistries at the covalent linkage site. *J. Med. Chem.* 31:583–590.

Chen, Q., F. N. Chowdhury, K. Maskos, and M. D. Barkley. 1994. Time-resolved fluorescence studies of tomaymycin bonding to DNA. *Biochemistry.* 33:8719–8727.

Chen, Q., W. J. Walczak, and M. D. Barkley. 1995. Excited-state proton transfer from solvent to aromatic carbons in tomaymycin. *J. Am. Chem. Soc.* 117:556–557.

DeVoe, H., and I. Tinoco, Jr. 1962. The stability of helical polynucleotides: base contributions. *J. Mol. Biol.* 4:500–517.

Hanlon, S., and G. Pack. 1994. Anomalous protonic equilibria in the minor groove of DNA. *Biophys. J.* 66:A154.

Hertzberg, R. P., S. M. Hecht, V. L. Reynolds, I. J. Molineux, and L. H. Hurley. 1986. DNA sequence specificity of the pyrrolo[1,4]benzodiazepine antitumor antibiotics. Methidiumpropyl-EDTA-iron(II) footprinting analysis of DNA binding sites for anthramycin and related drugs. *Biochemistry.* 25:1249–1258.

Hurley, L. H., C. Gairola, and M. Zmijewski. 1977. Pyrrolo(1, 4)benzodiazepine antitumor antibiotics. In vitro interaction of anthramycin, sibiromycin and tomaymycin with DNA using specifically radiolabelled molecules. *Biochim. Biophys. Acta.* 475:521–535.

Hurley, L. H., and D. R. Needham-VanDevanter. 1986. Covalent binding of antitumor antibiotics in the minor groove of DNA. Mechanism of action of CC-1065 and the pyrrolo(1,4)benzodiazepines. *Acc. Chem. Res* 19:230–237.

Hurley, L. H., T. Reck, D. E. Thurston, D. R. Langley, K. G. Holden, R. P. Hertzberg, J. R. E. Hoover, G. Gallagher, Jr., S.-M. Mong, and R. K. Johnson. 1988. Pyrrolo[1,4]benzodiazepine antitumor antibiotics: relationship of DNA alkylation and sequence specificity to the biological activity of natural and synthetic compounds. *Chem. Res. Toxicol.* 1:258–268.

Inman, R. B., and R. L. Baldwin. 1962. Helix-random coil transitions in synthetic DNAs of alternating sequence. *J. Mol. Biol.* 5:172–184.

Jin, R., and K. Breslauer. 1988. Characterization of the minor groove environment in a drug-DNA complex: bisbenzimide bound to the poly[d(AT)]·poly[d(AT)] duplex. *Proc. Natl. Acad. Sci. USA.* 85: 8939–8942.

Kizu, R., P. H. Draves, and L. H. Hurley. 1993. Correlation of DNA sequence specificity of anthramycin and tomaymycin with reaction kinetics and bending of DNA. *Biochemistry.* 32:8712–8722.

Knutson, J. R., J. M. Beechem, and L. Brand. 1983. Simultaneous analysis of multiple fluorescence decay curves: a global approach. *Chem. Phys. Lett.* 102:501–507.

Kohn, K. W., D. Glaubinger, and C. L. Spears. 1974. The reaction of anthramycin with DNA II. Studies of kinetics and mechanism. *Biochim. Biophys. Acta.* 361:288–302.

Kohn, K. W., and C. L. Spears. 1970. Reaction of anthramycin with deoxyribonucleic acid. *J. Mol. Biol.* 51:551–572.

Kolber, Z. S., and M. D. Barkley. 1986. Comparison of approaches to the instrumental response function in fluorescence decay measurements. *Anal. Biochem.* 152:6–21.

Kopka, M. L., D. S. Goodsell, I. Baikalov, K. Grzeskowiak, D. Cascio, and R. E. Dickerson. 1994. Crystal structure of a covalent DNA-drug adduct: anthramycin bound to C-C-A-A-C-G-T-T-G-G and a molecular explanation of specificity. *Biochemistry.* 33:13593–13610.

Lamm, G., and G. Pack. 1990. Acidic domains around nucleic acids. *Proc. Natl. Acad. Sci. USA.* 87:9033–9036.

Morgan, A. R., and R. D. Wells. 1968. Specificity of the three-stranded complex formation between double-stranded DNA and single-stranded RNA containing repeating nucliotide sequences. *J. Mol. Biol.* 37:63–80.

Mostad, A., C. Rømming, and B. Storm. 1978. Structure of the DNA complexing agent anthramycin. *Acta Chim. Scand.* B32:639–645.

Nishioka, Y., T. Beppu, M. Kohsaka, and K. Arima. 1972. Mode of action of tomaymycin. *J. Antibiot.* 25:660–667.

Petrusek, R. L., G. L. Anderson, T. F. Garner, Q. L. Fannin, D. J. Kaplan, S. G. Zimmer, and L. H. Hurley. 1981. Pyrrolo[1,4]benzodiazepine antibiotics. Proposed structures and characteristics of the in vitro deoxyribonucleic acid adducts of anthramycin, tomaymycin, sibiromycin, and neothramycins A and B. *Biochemistry.* 20:1111–1119.

Pierce, J. R., M. Nazimiec, and M.-S. Tang. 1993. Comparison of sequence preference of tomaymycin- and anthramycin-DNA bonding by exonuclease III and λ exonuclease digestion and UvrABC nuclease incision analysis. *Biochemistry.* 32:7069–7078.

Rao, S. N., U. C. Singh, and P. A. Kollman. 1986. Molecular mechanics simulations on covalent complexes between anthramycin and B DNA. *J. Med. Chem.* 29:2484–2492.

Remers, W. A., M. D. Barkley, and L. H. Hurley. 1992. Pyrrolo(1,4)benzodiazepines. Unraveling the complexity of the structures of the tomaymycin-DNA adducts in various sequences using fluorescence, ^{1}H-NMR, and molecular modeling. *In* Nucleic Acid Targeted Drug Design. C. L. Propst and T. J. Perun, editors. Marcel Dekker, New York. 375–422.

Remers, W. A., M. Mabilia, and A. J. Hopfinger. 1986. Conformations of complexes between pyrrolo[1,4]benzpdiazepines and DNA segments. *J. Med. Chem.* 29:2492–2503.

Wang, J.-J., G. C. Hill, and L. H. Hurley. 1992. Template-directed design of a DNA-RNA cross-linker based upon a bis-tomaymycin-duplex adduct. *J. Med. Chem.* 35:2995–3002.

Wells, R. D., J. E. Larson, R. C. Grant, B. E. Shortle, and C. R. Cantor. 1970. Physicochemical studies on polydeoxyribonucleotides containing defined repeating nucleotide sequences. *J. Mol. Biol.* 54:465–497.

Yanagi, K., G. E. Prive, and R. E. Dickerson. 1991. Analysis of local helix geometry in three B-DNA dodecamers and 8 dodecamers. *J. Mol. Biol.* 217:201–214.